Title
Communication—Functional Conductive Polymer Binder for Practical Si-Based Electrodes

Journal
Journal of The Electrochemical Society, 168(5)

ISSN
0013-4651

Authors
Zhu, Tianyu
Liu, Gao

Publication Date
2021-05-01

DOI
10.1149/1945-7111/abff01

Peer reviewed

Journal of The Electrochemical Society

Communication—Functional Conductive Polymer Binder for Practical Si-Based Electrodes

To cite this article: Tianyu Zhu and Gao Liu 2021 *J. Electrochem. Soc.* **168** 050533

Journal of The Electrochemical Society, 2021 **168** 050533

Communication—Functional Conductive Polymer Binder for Practical Si-Based Electrodes

Tianyu Zhu and Gao Liu[*,z]

Energy Storage & Distributed Resources Division, Lawrence Berkeley National Laboratory, Berkeley, California 94720, United States of America

Multifunctional conductive binders represent an emerging class of polymer materials to address inherent challenges of Si electrodes for high capacity lithium-ion batteries. Advanced binders with oriented functionalities are greatly desired to facilitate the battery chemistry. We here report stable capacity cycling of a practical composite anode comprising industrial available SiO_x (>60 wt%), carbon materials and a conductive polymer binder—poly(9,9-dioctylfluorene-*co*-fluorenonecomethylbenzoic ester) (PFM). This multifunctional polymer functions as both an interface modifier and an electrode binder for high-performing SiO_x composite electrodes. The viability of multifunctional conductive polymer binders was further validated in a practical full cell.
 [DOI: 10.1149/1945-7111/abff01]

Manuscript submitted February 21, 2021; revised manuscript received May 3, 2021. Published May 20, 2021.

There is broad usage of electrically conductive polymers in electrochemical systems, such as electroluminescence media,[1] organic electrodes,[2] conductive network,[3–5] surface modifiers and electrode binders.[3,4,6,7] The advantages of using these synthetic polymers come from their structural and chemistry versatilities,[8–10] which grants numerous possibilities to build conductive macromolecules with oriented functionalities for various electrochemical systems.

For silicon-based anode applications, the inherent challenges arise from both large volume expansion and Si surface instabilities (e.g. interfacial chemical reactions with electrolytes).[11–14] For instance, the volume change of Si materials during charge/discharge generates electrode level stress to fracture the composite electrodes, and further leads to the capacity decay and limited Coulombic efficiency.[15,16] Efforts have been made to develop nanosized Si materials (namely Si nanoengineering) to improve resistance to fracture during cycling.[17,18] Besides, many electrolytes and additives were developed to modify the interfacial reactions and improve the cycling Coulombic efficiency.[19,20] Using multifunctional binders for Si anodes has been proven as one of the most effective methods to address these dual challenges and meet practical needs with suitable cost.[7,21] Such conductive polymers were also designed to incorporate various functionalities to improve the mechanical and adhesion properties for surface coating.[22] The thin polymeric layers coated on the surface of Si materials are expected to be both uniform and strong, which can provide great interface protection from the electrolyte-involved reactions.[23] On the other hand, covalent bonding with the Si surfaces can provide superb adhesion property, which is favorable to combat the electrode level stress during cycling.[23–26] Furthermore, due to the redox-active nature for conductive polymers, the polymer layer is usually electrically active, which allows polymers to transform during the lithium alloying and dealloying with Si materials.[4] Finally, conductive polymers also modulate the solid electrolyte interface (SEI) growth during the electrochemical process, leading to a different type and more stable SEI than that only on the Si surface.[5,27–29]

We have previously demonstrated the superb Si nanoparticles with conductive polymer binders.[4,28,30] However, the cost of nanosized Si materials and the processing difficulties are the major issues inhibit commercialization. Herein, we report a composite electrode comprising high ratio of industry available SiO_x particles, graphite particles, acetylene black and a conductive polymer binder. This class of conductive polymer binder based SiO_x electrodes shows high reversible capacity and high Coulombic efficiency as well as excellent cycling stability. The viability of multifunctional conductive polymer binders for high-performing composite electrodes was further validated in a practical full cell.

Experimental

Materials.—All chemical reagents were purchased from Sigma-Aldrich and used as received. Poly(9,9-dioctylfluorene-co-fluorenonecomethylbenzoic ester) (denoted as PFM) was synthesized and purified according to the literature procedure.[4] Carbon-coated SiO_x material was obtained from Shinetsu. Graphite for electrode fabrication was purchased from Hitachi. Lithium iron phosphate ($LiFePO_4$, LFP) cathode was obtained from Argonne National Lab. Celgard 2400 separator was purchased from Celgard. Lithium-ion electrolyte (Gen 2) was obtained from the Argonne National Lab, containing 1.2M $LiPF_6$ in ethylene carbonate, ethylmethyl carbonate (EC/EMC = 3/7 w/w) with or without fluoroethylene carbonate (FEC) as an additive.

Electrode fabrication and cycling test.—SiO_x composite electrodes. A given amount of PFM polymer (or PVDF as comparison) binder was dissolved in specific amount of solvent to form a homogeneous and viscous solution. Then, SiO_x active material and graphite and Denka black were sequentially added and thoroughly ground for 30 min under room temperature. The weight ratios of PFM binder, SiO_x, graphite and Denka black are 15%, 60%, 20% and 5% respectively. The slurry was coated on a copper foil by using a doctor blade (~200 μm), and the coated electrode was then dried and baked at elevated temperatures in the vacuum oven, resulting in a mass loading of SiO_x to be 1.52 ± 0.12 mg cm^{-2}. The corresponding area capacity and volumetric capacity based on the electrode volume were determined to be around 2.40 mAh cm^{-2} and 597 mAh cm^{-3} (laminate thickness ~40 μm).

Coin cells (CR2032, MTI Corp.) were assembled in an argon-filled glovebox. The galvanostatic cycling performance of the assembled coin cells was evaluated with Maccor Series 4000 Battery Test system (MACCOR Inc. Tulsa OK, USA) in a thermal chamber at 30 °C. The C rate was determined based on the theoretical capacity upon a full lithiation of the active material (commercial SiO_x). The cut-off voltage of cell testing is between 1.0 V and 0.01 V for half-cell, and 3.35 V to 2.70 V for SiO_x/LFP full cell, assuming a theoretical capacity of 1,200 mAh g^{-1} for SiO_x and 135 mAh g^{-1} for LFP. The half-cells were galvanostatically cycled at a rate of C/10, while the full cells were pre-cycled at 48 mA g^{-1} (based on the amount of SiO_x active material) for 3 loops and at 120 mA g^{-1} for 10 loops before cycling at a rate of 120 mA g^{-1} or 600 mA g^{-1} for the following loops. The specific capacities reported in this work are calculated per gram of SiO_x, considering graphite,

*Electrochemical Society Member.
[z]E-mail: gliu@lbl.gov

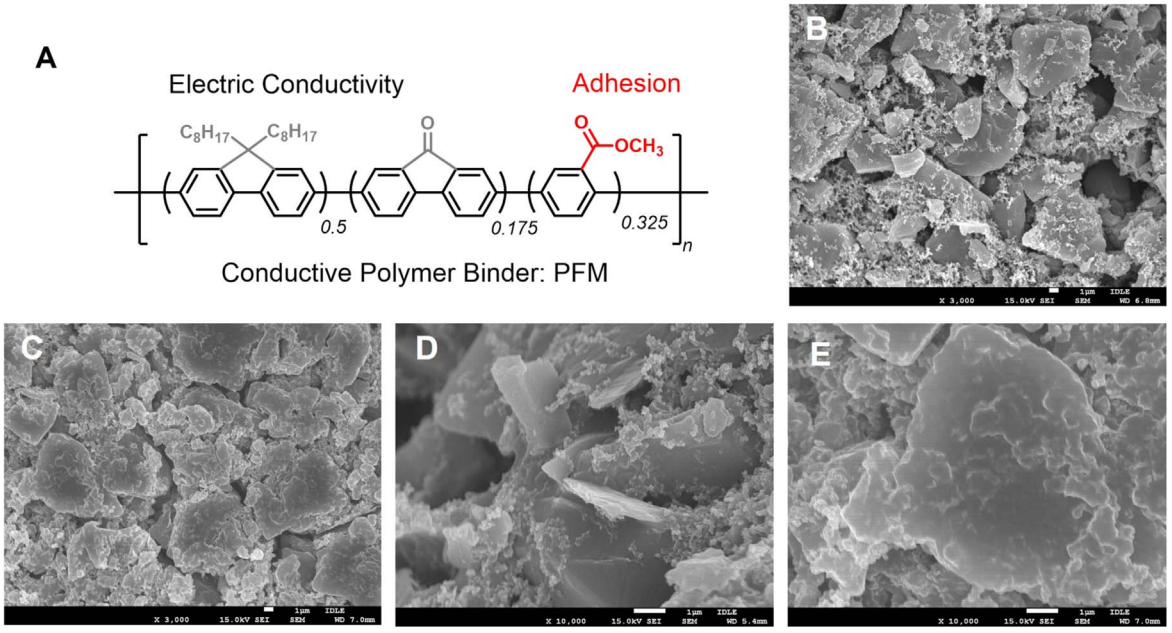

Figure 1. (A) Molecular structure of multifunctional PFM binder; SEM images of (B) the pristine high-loading SiO_x electrodes with PFM binder, (C) composite electrodes after 20 cycles (at a rate of C/10) at discharge state; (D) and (E) are higher magnification images for (B) and (C), respectively.

binder and Denka black only contributed to less than 10% of overall capacity. The full cell impedance was executed on a VSP300 potentiostat (Biologic, Claix, France) with frequency range was from 10 mHz to 100 kHz under ac stimulus with 10 mV of amplitude and no applied voltage bias. The full cell impedance was measured at a resting voltage of 3.12 V after 4 h resting, and ~50% state of charge (SOC).

Characterization.—The surface images of composite electrodes (or binder films) on the copper foil were collected with Scanning electron microscopy (SEM, JSM-7500F JOEL Ltd., Tokyo, Japan) with an accelerating voltage of 12 kV under high vacuum at room temperature.

Results and Discussion

Polymer binders play a critical role in functional composite electrodes, although they are mostly inactive towards electrochemical processes.[31–33] Unlike conventional binders (e.g. polyvinylidene fluoride), highly functionalized conductive binders can participate in electrochemical processes and provide multiple functionalities to the composite electrode. We have previously developed a multifunctional conductive polymer—PFM, as Si anode binders (Fig. 1A).[4] Generally, PFM has a highly conjugated polymer backbone to provide electric conductivity to the electrode matrix and to the surface of the Si-based materials, while the polar ester groups in the side-chains provide critical adhesion functions to the active materials (e.g. Si, SiO_2 or carbon surfaces). The chemical bonding between the particles and binders was characterized to be strong covalent bonds between Si and polymers.[6]

Equally important are the extended polymer structure and uniformity of the coating layers, which enables effective surface modification of the active materials.[34] In coating practice, priming is an important step is to allow uniform distribution of the bonding agents and the formation of strong adhesion force to the surface. The hydrophilic functional groups (e.g. hydroxide groups, oxygen rich functionalities) on electrode particles can serve as prime agents, while the ester groups on PFM can help to build strong chemical bonding during the coating process. The morphology of freshly prepared composite electrodes was imaged by SEM (Figs. 1B, 1D). Unlike PVDF binders forming polymer aggregates in the composite electrode, PFM binders (15 wt.%) were uniformly coated on the surface of the particles without forming any polymer aggregates. Based on the surface area for composite electrodes, the PFM coating was estimated to be 15 nm thick by covering the surface for all the particles.[26] In this case, the PFM coating layer is barely seen under SEM unless the polymers aggregate to form bigger chunks. Figure 1C, 1E show the SEM image of composite electrodes after cycling against Li counter electrodes for 20 cycles at a rate of C/10. No obvious electrode disruption was observed, suggesting the PFM binder effectively covers the surface and holds the active materials together. There is also minimum formation of electrolyte decomposition products after 20 cycles on the surface of active materials to cause the interface decay.

It's worth noting that the SiO_x loading in the composite electrodes was high (~60 wt.%). Typically, electrodes with such high SiO_x content show fast capacity fading in the cell testing due to the electrode mechanical failure and surface side reactions such as the electrode with PVDF binder in Fig. 2A.[16] The conductive binder used to modify the surface of active materials and bind them together was 15 wt.%. In the SiO_x electrode against Li metal half-cell testing, without FEC stabilizing additive in the electrolyte, the cell can cycle at full capacity for 20 cycles before it reaches fast fading stage (Fig. 2A). After the capacity drop to lower than 750 mAh g^{-1} (half of original capacity), the harvested electrode with a new lithium metal and standard electrolyte can still provide a capacity of 1500 mAh g^{-1} (nearly the full capacity of the SiO_x electrode). Both the capacity retaining in the first 20 cycles and recovery after in the harvest electrode indicate the superb adhesion and the surface protection effect of the PFM binder. In comparison, composite electrodes with PVDF binder (same loading of active materials) displays a rapid capacity decay and an early cell failure within only 10 cycles.

By simply adding 5 wt.% of FEC to the standard electrolyte, the half-cell with SiO_x electrode (against Li metal) shows remarkable cycling stability and high Coulombic efficiency (Fig. 2B). This improved cycling performance in half-cell study can partially attribute to the FEC stabilization effect to the Li metal counter electrode. Taken together, the combination of PFM binder as a surface modifier and FEC as an electrolyte additive enables excellent protection to the Si surface, which were difficult to passivate.

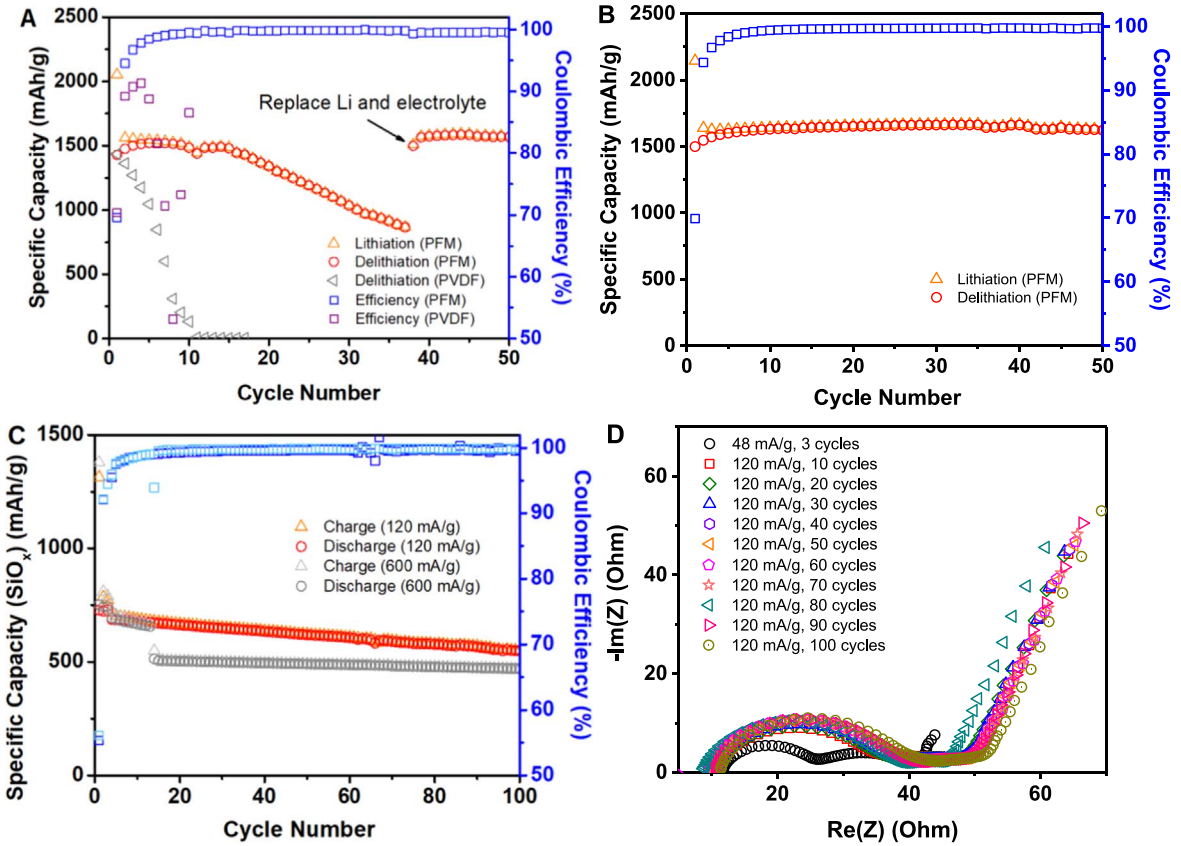

Figure 2. Galvanostatic cycling performance of SiO_x electrodes. SiO_x electrode against Li metal counter electrode using (A) Gen 2 electrolyte, (B) Gen 2 electrolyte and 5% FEC as an additive; (C) Full cell cycling performance of SiO_x anode and LPF cathode using Gen 2 electrolyte and 5% FEC as an additive. The capacity is reported based on SiO_x anode; (D) Impedance spectra of one typical SiO_x-LFP full cell at 3.12 V resting voltage towards 100 cycles.

Table I. Coulombic efficiency of SiO_x electrodes with conductive PFM binder against Li metal counter electrode and LPF cathode.

		Cycle number						
Counter electrode	FEC content	1st	2nd	5th	10th	20th	30th	50th
Li	0%	69.57	94.52	98.42	99.49	99.80	99.82	99.52
Li	5%	69.88	94.33	98.35	99.36	99.64	99.69	99.62
LFP	5%	55.32	92.09	97.53	98.71	99.31	99.51	99.64

The lithium-ion full cells with LFP cathode were assembled to further evaluate the electrochemical performance of the SiO_x composite electrode. The full cell shows stable cycling up to hundreds of cycles at a rate of 120 mA g^{-1} with only slight capacity drop (Fig. 2C, over 80% capacity retention after 100 cycles). Furthermore, the full cell also displays excellent rate capability, providing ~470 mAh g^{-1} after 100 cycles at a rate of 600 mA g^{-1}. It's noted that no prelithiation is applied to the system, the combined Li loss of SiO_x and PFM activation in the first cycle accounts for ~40% of the LPF capacity. Thus, the cell is only cycled at about 50% of full capacity for the SiO_x anode.

To gain the underlying reasons for excellent cell performance, electrochemical impedance spectroscopy (EIS) was conducted on full cells with the SiO_x composite electrode. It was found the cell impedance stabilized after formation cycles and only display neglectable increase in the subsequent 10 to 100 cycles (Fig. 2D). LFP cathode is routinely used as a standard electrode for the study of anode, due to the superb stability of LFP and flat potential across its capacity range. When the same SiO_x-LPF cell measured at the same cell voltage, the impedance spectra change reflects the changes of the SiO_x electrode. In this case, very small changes of the cell impedance are observed after the 10th cycles. This demonstrates the superb interfacial stability of the entire cell. Since the LFP is stable, the SiO_x interface is considered to be also very stable at least during the 100 cycles tested. Combining with the high Coulombic efficiency (Table I, >99.5%), and minimum electrolyte decomposition on the SiO_x surface (Fig. 1E), PFM stands out as a premium conductive binder for uniform Si surface modification and durable adhesion. Following efforts are devoted to combining new manufacturing technologies such as prelithiation to address other practical challenges and to allow the full utilization of Si-based electrode.

Summary

In summary, we present a conductive polymer binder to function as both surface modifier and binder for advanced Si-based electrodes. Specifically, PFM with exceptional mechanical stress tolerance, adhesion/cohesion properties and electric conductivity was demonstrated as a promising polymer binder for industry available Si materials. The electrochemical performance of the resulting composite electrodes was

evaluated in both half-cells against lithium metal and practical full cells against an LFP cathode. This work represents an important step towards understanding the surface modification of Si/carbon materials and developing high-performing composite electrodes through conductive binder design.

Acknowledgments

This research was funded by the Assistant Secretary for Energy Efficiency, Vehicle Technologies Office. Lawrence Berkeley National Laboratory is supported by the Director, Office of Science, Office of Basic Energy Sciences, of the US Department of Energy under contract no. DE-AC02-05CH11231.

ORCID

Tianyu Zhu https://orcid.org/0000-0001-9115-6462
Gao Liu https://orcid.org/0000-0001-6886-0507

References

1. Q. Pei, G. Yu, C. Zhang, Y. Yang, and A. J. Heeger, *Science*, **269**, 1086 (1995).
2. Y. Lu and J. Chen, *Nat. Rev. Chem.*, **4**, 127 (2020).
3. Y.-H. Huang and J. B. Goodenough, *Chem. Mater.*, **20**, 7237 (2008).
4. G. Liu, S. Xun, N. Vukmirovic, X. Song, P. Olalde-Velasco, H. Zheng, V. S. Battaglia, L. Wang, and W. Yang, *Adv. Mater.*, **23**, 4679 (2011).
5. H. Wu, G. Yu, L. Pan, N. Liu, M. T. McDowell, Z. Bao, and Y. Cui, *Nat. Commun.*, **4**, 1 (2013).
6. H. Zhao, Z. Wang, P. Lu, M. Jiang, F. Shi, X. Song, Z. Zheng, X. Zhou, Y. Fu, and G. Abdelbast, *Nano Lett.*, **14**, 6704 (2014).
7. M. Y. Wu et al., *J. Am. Chem. Soc.*, **135**, 12048 (2013).
8. T. Zhu, J. Zhang, and C. Tang, *Trends Chem*, **2**, 227 (2020).
9. S. Gao, F. Sun, A. Brady, Y. Pan, A. Erwin, D. Yang, V. Tsukruk, A. G. Stack, T. Saito, and H. Yang, *Nano Energy*, **73**, 104804 (2020).
10. M. Lis, K. Chudzik, M. Bakierska, M. Świętosławski, M. Gajewska, M. Rutkowska, and M. Molenda, *J. Electrochem. Soc.*, **166**, A5354 (2019).
11. Z. Xu, J. Yang, T. Zhang, Y. Nuli, J. Wang, and S.-I. Hirano, *Joule*, **2**, 950 (2018).
12. M. Al-Maghrabi, J. Suzuki, R. Sanderson, V. Chevrier, R. Dunlap, and J. Dahn, *J. Electrochem. Soc.*, **160**, A1587 (2013).
13. B. Liu, P. Soares, C. Checkles, Y. Zhao, and G. Yu, *Nano Lett.*, **13**, 3414 (2013).
14. Y. Shi, X. Zhou, and G. Yu, *Acc. Chem. Res.*, **50**, 2642 (2017).
15. H. Wang, J. Fu, C. Wang, J. Wang, A. Yang, C. Li, Q. Sun, Y. Cui, and H. Li, *Energy Environ. Sci.*, **13**, 848 (2020).
16. T. Liu, Q. Chu, C. Yan, S. Zhang, Z. Lin, and J. Lu, *Adv. Energy Mater.*, **9**, 1802645 (2019).
17. H. Kim, M. Seo, M. H. Park, and J. Cho, *Angew. Chem. Int. Ed.*, **49**, 2146 (2010).
18. Y. Yao, M. T. McDowell, I. Ryu, H. Wu, N. Liu, L. Hu, W. D. Nix, and Y. Cui, *Nano Lett.*, **11**, 2949 (2011).
19. Y. Li, K. Yan, H.-W. Lee, Z. Lu, N. Liu, and Y. Cui, *Nat. Energy*, **1**, 1 (2016).
20. J. Chen, X. Fan, Q. Li, H. Yang, M. R. Khoshi, Y. Xu, S. Hwang, L. Chen, X. Ji, and C. Yang, *Nat. Energy*, **5**, 386 (2020).
21. H. Chen, M. Ling, L. Hencz, H. Y. Ling, G. R. Li, Z. Lin, G. Liu, and S. Q. Zhang, *Chem. Rev.*, **118**, 8936 (2018).
22. T. Y. Zheng, Z. Jia, N. Lin, T. Langer, S. Lux, I. Lund, A. C. Gentschev, J. Qiao, and G. Liu, *Polymers*, **9**, 657 (2017), https://www.mdpi.com/2073-4360/9/12/657.
23. H. Zhao et al., *Nano Lett.*, **14**, 6704 (2014).
24. H. Zhao et al., *Nano Lett.*, **15**, 7927 (2015).
25. H. Zhao, Y. Wei, C. Wang, R. M. Qiao, W. L. Yang, P. B. Messersmith, and G. Liu, *ACS Appl. Mater. Interfaces*, **10**, 5440 (2018).
26. G. Liu, H. Zheng, X. Song, and V. S. Battaglia, *J. Electrochem. Soc.*, **159**, A214 (2012).
27. D. Liu, Y. Zhao, R. Tan, L. L. Tian, Y. D. Liu, H. B. Chen, and F. Pan, *Nano Energy*, **36**, 206 (2017).
28. S. J. Park, H. Zhao, G. Ai, C. Wang, X. Y. Song, N. Yuca, V. S. Battaglia, W. L. Yang, and G. Liu, *J. Am. Chem. Soc.*, **137**, 2565 (2015).
29. L. Luo, P. Zhao, H. Yang, B. Liu, J.-G. Zhang, Y. Cui, G. Yu, S. Zhang, and C.-M. Wang, *Nano Lett.*, **15**, 7016 (2015).
30. H. Zhao, A. Du, M. Ling, V. Battaglia, and G. Liu, *Electrochim. Acta*, **209**, 159 (2016).
31. Z. Li, Y. Zhang, T. Liu, X. Gao, S. Li, M. Ling, C. Liang, J. Zheng, and Z. Lin, *Adv. Energy Mater.*, **10**, 1903110 (2020).
32. T.-W. Kwon, J. W. Choi, and A. Coskun, *Chem. Soc. Rev.*, **47**, 2145 (2018).
33. P.-F. Cao, G. Yang, B. Li, Y. Zhang, S. Zhao, S. Zhang, A. Erwin, Z. Zhang, A. P. Sokolov, and J. Nanda, *ACS Energy Lett.*, **4**, 1171 (2019).
34. Y. Shi, J. Zhang, L. Pan, Y. Shi, and G. Yu, *Nano Today*, **11**, 738 (2016).